

Scalings of domain wall energies in two dimensional Ising spin glasses

C. Amoruso,¹ E. Marinari,¹ O. C. Martin,² and A. Pagnani²

¹Dipartimento di Fisica, SMC and UdR1 of INFN, INFN,
Università di Roma La Sapienza, P.le Aldo Moro 2, 00185 Roma, Italy.

²Laboratoire de Physique Theorique et Modeles Statistiques,
bât. 100, Université Paris-Sud, F-91405 Orsay, France.

(Dated: March 22, 2024)

We study domain wall energies of two dimensional spin glasses. The scaling of these energies depends on the model's distribution of quenched random couplings, falling into three different classes. The first class is associated with the exponent $\phi = 0.28$, the other two classes have $\phi = 0$, as can be justified theoretically. In contrast to previous claims we find that $\phi = 0$ does not indicate $d = d_1^c$ but rather $d < d_1^c$, where d_1^c is the lower critical dimension.

PACS numbers: 75.10.Nr, 75.40.Mg, 02.60.Pn

Spin glasses [1] exhibit many subtle phenomena such as diverging non-linear susceptibilities, aging and memory, making it a real challenge to understand these materials. In spite of much work, there is still no consensus even on the nature of the frozen order in equilibrium. More surprising still, the case of two dimensions also is not completely understood. In particular, the scaling of the stiffness, a cornerstone of spin glass theory, is different when the spin-spin couplings are of the form $J_{ij} = 1$ compared to when they have a Gaussian distribution [2]. This has been confirmed since using more powerful numerical techniques [3, 4], and in fact it was interpreted in [4] as a lack of universality, but this is unexpected and unexplained. Here we solve this puzzle: we find that different types of quenched disorder lead to three distinct behaviors. In particular, we motivate why the class of models that includes the case $J_{ij} = 1$ gives for the stiffness exponent $\phi = 0$, and we explain what tells us about the lower critical dimension.

The model, its properties and our methods | The model consists of $N = L^2$ Ising spins $S_i = \pm 1$ on a simple square lattice with periodic boundary conditions. The Hamiltonian is

$$H = - \sum_{\langle ij \rangle} J_{ij} S_i S_j; \quad (1)$$

where the sum runs over all pairs of nearest neighbors $\langle ij \rangle$ and the J_{ij} are the quenched random spin-spin couplings. We shall consider different distributions of these couplings, all of which are symmetric about $J = 0$. We begin with continuous distributions; most common is the one where the J_{ij} are Gaussian random variables with zero mean and unit variance. After that we investigate discrete distributions; the most common distribution of this type has $J_{ij} = \pm 1$ with equal probability.

An important feature of spin glass ordering is the spin glass stiffness; the corresponding exponent ϕ describes how excitation free energies scale with the associated length scale. The standard way to measure this exponent is via the change in the system's free energy when

going from periodic to anti-periodic boundary conditions. At $T = 0$ this reduces to measuring the difference

$$E = E_0^{(P)} - E_0^{(AP)}; \quad (2)$$

where $E_0^{(P)}$ and $E_0^{(AP)}$ are the ground state energies for the system with respectively periodic and anti-periodic boundary conditions say in the x direction. We are interested in the probability distribution of E when considering an ensemble of J_{ij} and in the scaling law of its standard deviation σ_E :

$$\sigma_E \propto L^{-\phi}. \quad (3)$$

Measurements of ϕ in two dimensional spin glasses (see for instance [2]) give $\phi = 0.28$. However, for the $J_{ij} = 1$ distribution, Hartmann and Young [4] recently showed that σ_E remains of $O(1)$ for increasing L , implying that in this case $\phi = 0$. In dimension d above the lower critical dimension d_1^c we have $\phi > 0$ and spin glass ordering is stable against thermal fluctuations. On the contrary, when $\phi < 0$, thermal fluctuations prevent spin glass ordering. Because of this, the authors of [4] conjectured that $d_1^c = 2$ for the $J_{ij} = 1$ model. We shall see that d_1^c should be identified with the highest value of d where $\phi = 0$, and so in fact $d_1^c = 2.5$ as believed before the study in [4].

In this work we address these questions by first determining numerically the properties of $P(E)$ and then by using the real space renormalization group picture. For the first part, we compute the ground states of our systems using a heuristic algorithm [5]. In practice, when the lattice is not too large ($L \leq 80$), the algorithm returns the ground state with a high level of confidence for all of the distributions we shall consider in this work. The problem is to reduce enough the statistical errors; in practice we used a few tens of thousands of samples at a few values of L for each case.

Class 1: "continuous" distributions | We first focus on distributions $P(J)$ that include a continuous part (we shall see later that this class includes certain discrete

distributions also). When L is sufficiently large, E can then take on arbitrary values. The value of ΔE for continuous distributions is well known only for Gaussian J_{ij} ; in fact we are aware of no tests of universality in $d = 2$, though the standard lore is that both ΔE and the shape of $P(jE \neq E)$ are universal [2].

In a first series of runs we obtained $P(E)$ and E for the model with Gaussian couplings. Then we moved on to a continuous yet singular probability density $P(J_{ij})$: $P(J_{ij} = J) = f P_1(J) + (1-f) P_2(J)$, where $P_1(J) = \frac{e^{-\frac{(J-1)^2}{2}} + e^{-\frac{(J+1)^2}{2}}}{2}$, $P_2(J) = \frac{1}{2} [(J-1)+ (J+1)]^{-2}$, and f is a measure of the height of the distribution at $J = 0$. We refer to this $P(J_{ij})$ as the broadened bimodal (BB) distribution since it reduces to the $J_{ij} = \pm 1$ distribution when $f = 0$.

In Fig. 1 we show E as a function of L when $P(J_{ij})$ is: (1) a Gaussian of zero mean and unit variance (GAUSS data); (2) the BB distribution, with $f = 0.1$ (BB 0.1 data); (3) as in (2) but with $f = 0.2$ (BB 0.2 data); (4) Gaussian but with the part in the interval $[-0.5; 0.5]$ forced to be 0 (HOLE data). Note that this last distribution has a large gap around $J_{ij} = 0$. In the

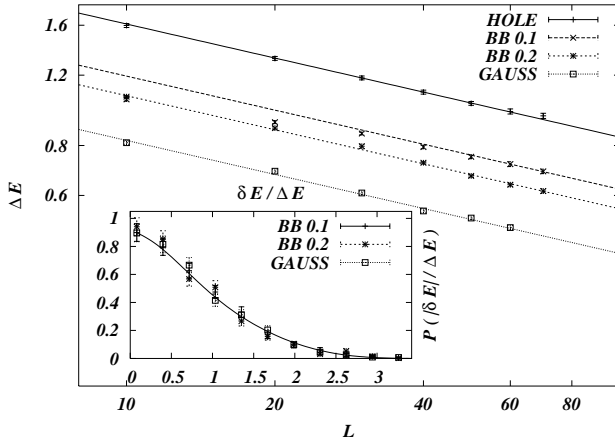


FIG. 1: E as a function of the system size for four different J_{ij} distributions. Straight lines are best one-parameter fits of the form $\text{const } L^{-0.282}$. Inset: the probability distribution $P(jE \neq E)$ at $L = 40$ for three of these distributions.

Gaussian case the power law scaling of E can be determined with good accuracy already from quite small lattices; fits to these data lead to $\alpha = 0.282 \pm 0.004$, in agreement with previous work. The distributions (2), (3) and (4) give rise to a similar scaling albeit only at larger L values. We have also considered other distributions such as $P(J_{ij})$ uniform in $[-1.5; 0.5]$ $[0.5; 1.5]$ (notice that this distribution also has a gap around $J = 0$), obtaining similar results. It thus seems very reasonable to expect that all distributions with a continuous part will lead to the same exponent, $\alpha = 0.28$.

A second universality issue concerns the shape of $P(E)$. In the inset of Fig. 1 we show the probabil-

ity density $P(jE \neq E)$ when $L = 60$ for the BB 0.1, BB 0.2, and GAUSS data: the different data sets basically coincide within statistical errors, strengthening the claim that in this class the distribution of domain wall energies is universal (the curve displayed is just to guide the eye).

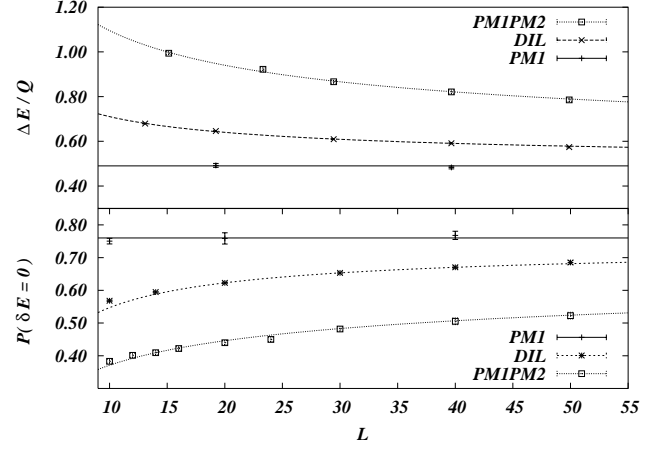


FIG. 2: E/Q (top) and $P(E = 0)$ (bottom) as a function of the system size for three discrete J_{ij} distributions: ± 1 (PM1), diluted ± 1 (DIL), and $\pm 1, \pm 2$ (PMIPM2).

Class 2: quantized energies | At variance with the former distributions, the $J_{ij} = \pm 1$ model leads to 0 [4]. We show in Fig. 2 that in this model E saturates quickly as L grows. Is the $J_{ij} = \pm 1$ model a special case, a class on its own? The crucial point is that the possible E values are quantized: E is always a multiple of a quantum Q , here $Q = 4$. This led us to consider distributions other than the ± 1 one with this same quantization property. We begin by "diluting" the $J_{ij} = \pm 1$ model, setting $J_{ij} = 0$ with probability 0.2. The main effect of this is to reduce the quantum from 4 to 2; indeed, the local fields now can take the value 0, 1, 2, 3, 4 instead of 0, 2, 4. In Fig. 2 we see that for this model (DIL data)

E seems to saturate, so again $\alpha = 0$. However the convergence is slow. In any renormalization group picture this convergence is governed by a "correction to scaling" exponent β . We assume $\beta = 0$ and that the asymptotic value of E is a non-zero constant given by the $J = \pm 1$ data; then we fit the diluted (DIL) model to the form:

$$E(L) = E(L = 1) + AL^{-\beta} \quad (4)$$

with A and β adjustable parameters. We have also considered distributions where $J_{ij} = J_1$ or J_2 with equal probability (we have studied the cases $J_2 = J_1 = 1.5, 2$ and 3). Again we find the convergence to be slow but fits as in (4) work well; furthermore, all the estimates of β are similar, being in the $[0.4; 0.6]$ interval. All these facts justify the claim that $\alpha = 0$ whenever E is quantized.

Just as in the continuous case, to analyze the shape of the distribution of E we must choose a scale; the cor-

rect choice is to compare the histograms after measuring all energies in units of the basic quantum Q . To test whether the histograms for the different J_{ij} distributions become identical in the large L limit we plot in Fig. 2 (lower panel) the probability $P(E=0)$ to find a zero energy domain wall. The data suggest that the histograms become identical in the large L limit, i.e., they support universality. (Following Eq. (4), we fix the asymptotic value of $P(E=0)$ to be that given by the $J=1$ model, and then we determine β ; in the plot we show these fits; they are all good and the values of β are close to 0.5.) We have checked in detail that this claim applies to the quantized distributions mentioned before and to the DIL model with 10% dilution.

Class 3: quantized energies revisited | So far we have only considered situations with even values of L . If L is odd (and the $J_{ij} = 1$), the possible values of $E=J$ are $2; 6; 10; \dots$. The quantum Q is still the separation between the energy values, but the positions of the histogram entries are different (in particular, $E=0$ is not allowed). A somewhat trivial consequence of this is that necessarily $\beta=0$ as $E=Q$ is greater or equal to $1=2$ for all L . Consider now the question of the universality of the histograms. We have checked within our error bars that the large L limit of $P(E=Q)$ for the $J_{ij} = 1$ model is the same as that obtained using the $J_2=J_1=3$ model (still with L odd of course). This kind of quantization thus gives rise to a third class, again with $\beta=0$.

Could there be further classes with quantized energies? Since we have imposed reflection symmetry of the distribution of the J_{ij} the only possible histograms are the two we discussed: E is a multiple of the quantum Q or of the form $(n+1/2)Q$, where n is integer. If the universality class depends only on the possible histogram types, then no other classes arise.

Discrete does not mean quantized | Let us also consider the case where the couplings are discrete but where there is no quantization. We consider the distribution $P(J) = \frac{1}{4}[(J-J_1) + (J-J_2)]$ (IRR for "irrational" hereafter), where $J_1 = 1$ and $J_2 = \frac{1+\sqrt{5}}{2} \approx 1.618$ is the golden mean. Clearly we have $E = 2(nJ_1 + mJ_2)$ where n and m are integers. Since $J_2=J_1$ is irrational, the set of possible E values becomes dense when $L \rightarrow \infty$ and so it is natural to conjecture that this $P(J_{ij})$ leads to domain wall energies in class 1. Our findings are that β decreases with L and shows no sign of saturation, and a power law fit gives $\beta = 0.29 \pm 0.01$, the value associated with class 1. Our conjecture is thus substantiated by these findings.

The convergence of $P(E=E)$ to its limit is more problematic: for finite L , the distribution is the sum of a finite number of delta functions: we can only hope to have a "weak convergence" to the P obtained with the Gaussian couplings. In these conditions it is appropriate to consider the integrated probability distribution

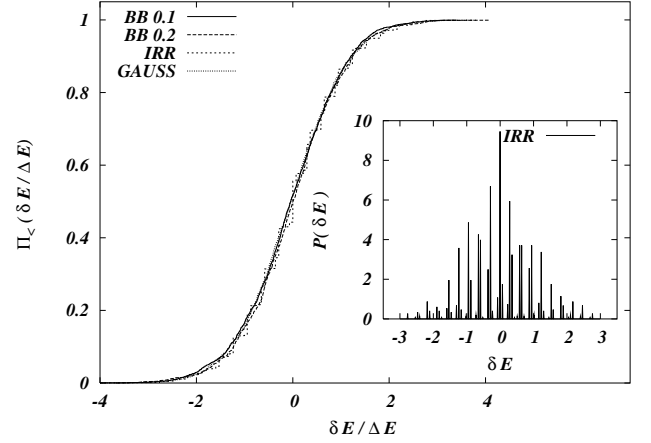


FIG. 3: The integrated probability distribution for $E = E$ in the Gaussian case, in the two BB cases, and in the irrational $J_2=J_1$ case ($L = 60$). Inset: binned probability distribution of $E = E$ for the irrational case (IRR), $L = 60$.

$\langle X \rangle = \frac{R_X}{1} P \frac{E}{E} d \frac{E}{E}$. In Fig. 3 we plot $\langle X \rangle$ for the irrational and for some continuous cases. The plots are very similar, supporting the claim that the discrete distribution IRR leads to domain wall energies in class 1. We have also included $P(E=E)$ as an inset into Fig. 3: we have used a small bin size that allows one to observe the complex structure.

The case of hierarchical lattices | The effect of having quantized E can also be studied on hierarchical lattices. One advantage is that one can study very large sizes, a second is that one can access a continuous range of dimensions. We have focused on Migdal-Kadanoff lattices [6]; these are obtained by recursively "expanding" graphs. Starting with one edge connecting two sites, one replaces it by b paths in parallel, each composed of s edges in series, leading to bs new edges. This procedure is repeated hierarchically; after G "generations" the distance between the outer-most spins is $L = s^G$, while the number of edges of the lattice is $(b^G s^G)$. The dimension of these lattices is $d = 1 + \ln(b)/\ln(s)$. One puts an Ising spin on each site and a coupling J_{ij} on each edge. Periodic boundary conditions simply imply that the two end spins must have the same value, and from this we define E .

The probability distribution of E can be followed from G to $G+1$. The recursion equations for $P(E)$ make sense for any s [7]: s can be an integer but it can also be any positive real value! One may then compute for an interval of dimensions, using either continuous J_{ij} (for instance to check universality [8, 9]) or quantized J_{ij} couplings (our focus here).

In Fig. 4 we show β as a function of dimension d (s is variable, b is fixed and set to 3). We show the values for continuous distributions and for when the quantization is of the form of class 3. As expected, if in one class $\beta > 0$, all classes lead to the same value of β , i.e., quantization

is irrelevant when the energy scale diverges. However, as soon as $\beta < 0$ in the continuous case, quantization gives rise to a histogram fixed point distribution in which the $j E_j$ are concentrated on the few lowest values and $\beta = 0$.

Similar results are obtained for class 2 quantization but there is an interesting difference. Indeed, since E can be zero in this class, one sees two further fixed points. An obvious one is associated with having $P(E = 0) = 1$, i.e., all domain wall energies vanish. It is easy to see that this fixed point is stable and has $\beta = 1$; there is no spin glass stiffness, and the system is paramagnetic even at zero temperature. The other fixed point is unstable and has $\beta = 0$. What is the interpretation of these two extra fixed points? To allow E to be zero, one can think of the diluted model where some of the bonds have $J_{ij} = 0$. Clearly when the dilution is strong enough, the non-zero bonds will no longer percolate and we are in a strongly paramagnetic phase; the renormalization group (RG) flow in this phase takes one to the $P(E = 0) = 1$ fixed point. On the contrary, at low dilution, we are in a spin glass phase and the RG flows are towards the other stable fixed point. On the boundary of these two phases, the RG flows takes one to another fixed point which is unstable: it is associated with the paramagnetic to spin glass transition as dilution is decreased. Such considerations have previously been developed for $d = 3$ Migdal-Kadanoff lattices [10].

Finally, we see that it is appropriate to define the lower critical dimension d_L^c from the end point of the $\beta = 0$ curve; $\beta = 0$ on its own does not signal $d = d_L^c$.

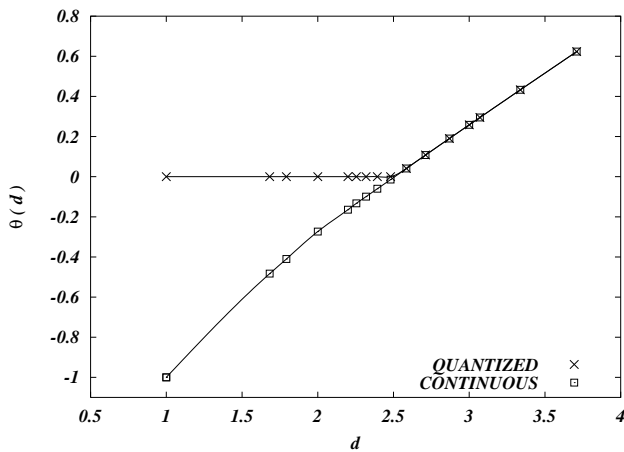


FIG. 4: β as a function of d for a one-parameter family of Migdal-Kadanoff lattices; we display two sets of data points, one for continuous J_{ij} distributions, the other for quantized distributions.

Discussion | Our numerical evidence of universality (both for β and $P(E = E)$) is very strong for continuous and related distributions (see figures 1 and 3). But we also find universality classes when E is quantized. This

classification is substantiated by the behavior of β and of the fixed point distributions of domain wall energies in Migdal-Kadanoff lattices. It is appropriate however to be cautious and to remark that the correction to scaling exponent ν we measure (see equation 4) is small, $\nu \approx 0.5$. Because of that we are not able to completely exclude the Bray and Moore expectation that $E(L = 1) = 0$ [11]. Our most extensive data are for the model D II with $f = 0.2$. Here our results give $E(L = 1) = Q = 0.49(1)$ while if we force $E(L = 1) = 0$, the χ^2 of the fit increases by 2.3; thus $E(L = 1) = 0$ is not excluded by our data though it appears as much less likely.

What is the source of the universality we observe? In the Migdal-Kadanoff lattices, the renormalization group transformation is clear and so the different classes are very natural. For the Euclidean lattices the existence of a renormalization group transformation for E has not been established, but since our data point to universality, it should be possible to define such a transformation. Note that its fixed point (and thus $P(E = E)$) will depend on the aspect ratio and on the fact that we use periodic boundary conditions. Our $P(E)$ are thus a priori not comparable to those of [4] where one of the directions had free boundary conditions.

We acknowledge important conversations with Giorgio Parisi that led us to this study, and we thank J.-P. Bouchaud for his comments. AP acknowledges the financial support provided through the European Community's Human Potential Programme under contract HPRN-CT-2002-00307, DYGLAGEMEM.

-
- [1] M. Mezard, G. Parisi, and M. A. Virasoro, Spin-Glass Theory and Beyond, vol. 9 of Lecture Notes in Physics (World Scientific, Singapore, 1987).
 - [2] A. J. Bray and M. A. Moore, in Heidelberg Colloquium on Glassy Dynamics, edited by J. L. van Hemmen and I. Morgenstern (Springer, Berlin, 1986), vol. 275 of Lecture Notes in Physics, pp. 121-153.
 - [3] N. Kawashima and H. Rieger, Europhys. Lett. 39, 85 (1997).
 - [4] A. K. Hartmann and A. Young, Phys. Rev. B 64, 180404 (2001), cond-mat/0107308.
 - [5] J. Houdayer and O. C. Martin, Phys. Rev. E 64, 056704 (2001), cond-mat/0105617.
 - [6] B. W. Southern and A. P. Young, J. Phys. C 10, 2179 (1977).
 - [7] E. M. F. Curado and J.-L. Meunier, Physica A 149, 164 (1988).
 - [8] E. Nogueira, Jr., S. Coutinho, F. Nobre, and E. Curado, Physica A 257, 365 (1998).
 - [9] S. Boettcher, cond-mat/0303431.
 - [10] A. J. Bray and S. Feng, Phys. Rev. B 36, 8456 (1987).
 - [11] A. J. Bray and M. A. Moore, Phys. Rev. Lett. 58, 57 (1987).